



# Microstructural refinement in spark plasma sintering 3Y-TZP nanoceramics



Chong Liu<sup>a</sup>, Mingyu Xiang<sup>b</sup>, Zhengyi Fu<sup>b</sup>, Zhijian Shen<sup>c</sup>, Yan Xiong<sup>a,\*</sup>

<sup>a</sup> Collaborative Innovation Center for Green Light-weight Materials and Processing, Hubei Province Key Laboratory of Green Materials for Light Industry, Hubei University of Technology, 430068 Wuhan, PR China

<sup>b</sup> State Key Lab of Advanced Technology for Materials Synthesis and Processing, Wuhan University of Technology, Wuhan 430070, PR China

<sup>c</sup> Department of Materials and Environmental Chemistry, Arrhenius Laboratory, Stockholm University, S-106 91 Stockholm, Sweden

## ARTICLE INFO

### Article history:

Received 20 November 2015

Received in revised form 21 February 2016

Accepted 17 March 2016

Available online 22 March 2016

### Keywords:

Spark plasma sintering (SPS)

Densification

Grain growth

Microstructural refinement

Particle rearrangement

## ABSTRACT

A commercial 3Y-TZP nanopowder was consolidated by spark plasma sintering (SPS) techniques. By special die-upset designs, each possible influence from the electric field, uniaxial pressure and heating rate was peeled to identify its contribution. Besides density and grain growth, the evolution of pore structure was consulted to clarify the relationships between microstructural development and densification kinetics. The results showed that neither electric current nor fast heating had no decisive contributions while external force was a necessity for the microstructural refinement. The authors proposed that the essentially underlying mechanism was the intensive particle rearrangement, which involves no grain growth but particle close-packing through grain rotation and sliding. The full advantages of this mechanism can be taken in rapid heating conditions, which combined with the application of higher pressures, make the SPS family of techniques to have advancement in the preparations of nanoceramics over their conventional counterparts characterized by slow heating features.

© 2016 Elsevier Ltd. All rights reserved.

## 1. Introduction

Spark plasma sintering (SPS) technique nowadays has attracted increasing attentions not only for nanoceramic processing but also in exploring the mechanisms underlying fast sintering. [1–3] Different from conventional irradiating, SPS involves a pulsed electric current passing directly through the graphite die, by which results in much faster heating rate as well as the controversial contributions from electric field or/and plasma. Similar to that in conventional hot press (HP), SPS also involves the application of a uniaxial but higher pressure for densification promotion and as high as 1 GPa pressure can be loaded using the high-pressure die setup [4,5]. Generally, the rapid densification of SPS has been considered resulting from the joint actions contributing from rapid heating, temperature, pressure, and plausibly electric field. Those flexible parameters, on the one hand, open up much more possibilities for microstructural manipulating that have never been achievable by conventional sintering techniques. On the other hand, the involving several parameters in SPS also makes the investigation of densification mechanisms rather complicated. Although

possible contributions from plasma [6], electric field [7], heating rate [8], and pressure [9] have been widely investigated, a universal explanation for the rapid densification achievable by SPS is still unavailable.

The authors' previous works have reported that, in SPS conditions, the dynamic pore coalescence in high-density regimes (>93% of theoretical density, TD) could be effectively suppressed [10,11]. Such microstructural refinement facilitated the low-temperature SPS sintering by yielding the fabrication of transparent nanoceramics [12]. The present study aims to clarify the underlying mechanism(s) of microstructural refinement in nonconductive nanoceramic SPS sintering. By special experimental designs, the possible parameters (electric field, heating rate and pressure) were separately peeled and the typical microstructural prototypes yielded from each different condition were compared. Present investigation will be expected to construct the status of the present understanding that the advantages of SPS are either overstated by overestimating the contribution of spark and plasma or overlooked by underestimating unique features established in SPS process.

## 2. Experiments

A commercial zirconia powder doped with 3 mol% yttria (TZ-3Y-E, Tosoh Co., Ltd., Tokyo, Japan) was used as the raw material.

\* Corresponding author.

E-mail address: [xiongyan1980@hotmail.com](mailto:xiongyan1980@hotmail.com) (Y. Xiong).

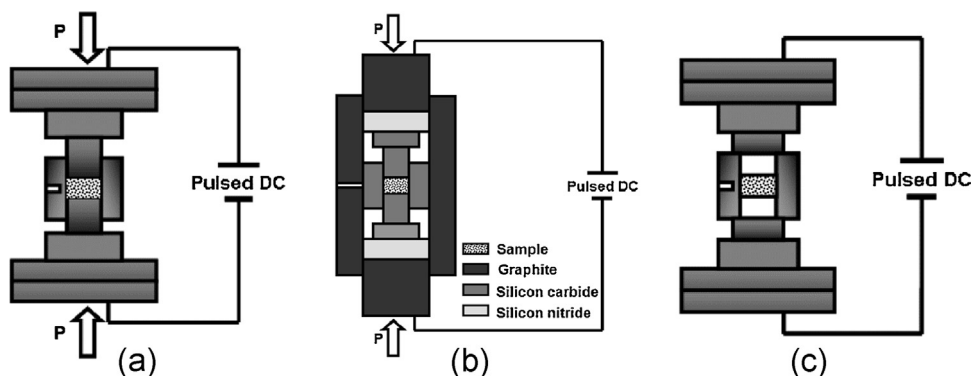


Fig. 1. Schematic mold designs in the present cycles for (a) conventional SPS, (b) high-pressure SPS and (c) pressureless SPS.

As received powder is in the form of spherical granules with the diameter ranging from 60 to 120  $\mu\text{m}$  formed by thermal spray drying particles with initial crystallite size of 27 nm calculated by X-ray diffraction (XRD) peak broadening. SPS sintering was carried out in Dr. Sinter 2050 apparatus (SPS Syntex Inc., Tokyo, Japan) in vacuum less than 6 Pa. Three different die-set designs were schemed as shown in Fig. 1.

- (1) Conventional SPS sintering. Each batch of 0.8 g as-received powder was poured into the cylindrical graphite die with an inner and outer diameter of 12 mm and 30 mm, respectively. A uniaxial pressure was automatically loaded to 20–100 MPa during the initial 3 min and kept constant to the end of each sintering cycle. The temperature was measured and regulated by a pyrometer focusing on the surface of graphite die. The temperature was firstly automatically raised to 600  $^{\circ}\text{C}$  in 3 min and then to the targeting temperatures at a heating rate of 10–300  $^{\circ}\text{C}/\text{min}$ .
- (2) High-pressure SPS (abbreviated as HP-SPS). The matryoshka-die developed by Munir's group [4], seen in Fig. 1(b), was adopted in present study. Two silica nitride pellets were used to isolated possible influences from electric field or/and plasma. Powder loading as well as following sintering were the same as the conventional SPS processes.
- (3) Pressureless SPS sintering (abbreviated as PL-SPS). The same graphite die of 12 mm inner diameter equipped with two  $\Phi 20$  mm punches were used to eliminate any external force on the sample during sintering as schemed in Fig. 1(c) [13]. 1.0 g powder was firstly shaped in a steel mold under 5 MPa pressure and further experienced 200 MPa cold-isostatic pressing (CIP) treatment. As obtained pellets have 49.7% of theoretical density (TD) and positioned in the middle of the die using graphite paper. The monitor and regulation of sintering temperature was the same as described above.

The relative density was measured by Archimedes method taking 6.08 g/cm<sup>3</sup> as the theoretical density of 3Y-TZP ceramics. Scanning electron microscopy (SEM) was used to characterize the microstructural evolution during sintering. To avoid possible artefacts, the mechanically grinded cross-sections were further polished using argon ion milling (Model SM-09010, Cross-section polisher, JEOL Co., Ltd., Tokyo, Japan), which was operated at 5 kV/90  $\mu\text{A}$  for 10 h. The ion-milled surfaces were further annealed at 950  $^{\circ}\text{C}$  for 60 min in air to expose the grain boundaries before SEM observations. Intercept method based on SEM images was used for the measurement of grain size. Pore size was characterized by both mercury intrusion method (Pascal 440, Porotec, Hofheim, Germany) and by defining the maximum pore size based on microstructural observations [10].

### 3. Results and discussion

The relative density and grain size evolutions under the 20 MPa and 100 MPa conventional SPS conditions were presented in Fig. 2, revealing that the grain growth was initiated at  $\sim 1100$   $^{\circ}\text{C}$  in both cases. Based on the data, different sintering cycles were performed as summarized in Table 1. It was shown that the SPS regime of 60 min soaking at 1100  $^{\circ}\text{C}$  under 100 MPa pressure yielded the final density higher than 99.5% of theoretical density (TD) the finest microstructures of the average grain size of less than 100 nm.

The microstructural evolutions during three different sintering cycles were investigated as shown in Fig. 3. Besides the mostly consulted two factors, relative density and grain size, the maximum pore size was also introduced to reveal the microstructural refinement during SPS process. As shown in Fig. 3(a), the maximum pore size experienced only slightly enlargement, from  $\sim 50$  nm up to  $\sim 180$  nm, in SPS conditions. Those residual pores could be eliminated by extended 60 min soaking at 1100  $^{\circ}\text{C}$  under constant 100 MPa pressure. By contrast, the maximum pores size even in the  $\sim 87\%$  TD partly densified samples dramatically increased by  $\sim 10$  times in both 1100  $^{\circ}\text{C}$  soaking and slow heating process of further pressureless consolidation, seen in Fig. 3(b) and (c). Due to the rather moderate grain-boundary diffusion at 1100  $^{\circ}\text{C}$ , those dynamically amplified pores could only be removed by increasing temperatures, seen in Fig. 3(c), yielding the grain growth blooming.

Those results indicated that the dynamic pore amplification had been the main obstacle for the preparation of 3Y-TZP nanoceramics from the present initial powder. The presence of external force might be a necessity for the suppression pore-enlargement. Similarly, the sample densified by HP-SPS also exhibited the satisfying density and grain size in final product using the same sintering parameters, seen in Table 1. The slightly larger grain size could be attributed to the higher sintering temperature resulted from the thicker walls of high-pressure die setup. In this case, possible effect(s) from either spark plasma or electric field were totally eliminated by the inserted silicon nitride disks. Such pore suppression was also observed during SPS heating by Trunec et al. using the similar high-pressure die setup [14]. In those regards, it could be reasonable to induce that possible effect(s) from neither spark plasma nor electric current might had no decisive contributions to microstructural refinement of spark plasma sintering.

The influence of fast heating on the microstructural refinement in SPS was consulted using the PL-SPS die setup. In this case, a much faster heating rate of 300  $^{\circ}\text{C}/\text{min}$  was applied and the possible contributions from external force were completely cancelled. As shown in Table 1, the CIPed green bodies could be fully densified after 60 min soaking in conventional pressureless sintering at 1350  $^{\circ}\text{C}$ , yielding the final average GS of  $\sim 240$  nm. The microstructural evolutions of the corresponding PL-SPSed samples were revealed in

Download English Version:

<https://daneshyari.com/en/article/1473463>

Download Persian Version:

<https://daneshyari.com/article/1473463>

[Daneshyari.com](https://daneshyari.com)